Effective conductivity of hard-sphere dispersions

C. A. Miller
Department of Mechanical and Aerospace Engineering, North Carolina State University, Raleigh, North Carolina 27659-7910

S. Torquato[a)]
Departments of Mechanical and Aerospace Engineering and of Chemical Engineering, North Carolina State University, Raleigh, North Carolina 27659-7910

(Received 21 May 1990; accepted for publication 30 July 1990)

Three-point bounds on the effective conductivity σ_e of isotropic two-phase composites, that improve upon the well-known two-point Hashin–Shtrikman bounds [J. Appl. Phys. **23**, 779 (1962)], depend upon a key microstructural parameter ζ_2. A highly accurate approximation for σ_e developed by Torquato [J. Appl. Phys. **58**, 3790 (1985)] also depends upon ζ_2. This paper reports a new and accurate algorithm to compute the three-point parameter ζ_2 for dispersions of hard spheres by Monte Carlo simulation. Data are reported up to values of the sphere volume fraction ϕ_2 near random close-packing and are used to assess the accuracy of previous analytical calculations of ζ_2. A major finding is that the exact expansion of ζ_2 through second order in ϕ_2 provides excellent agreement with the simulation data for the range $0 \leqslant \phi_2 \leqslant 0.5$, i.e., this low-volume-fraction expansion is virtually exact, even in the high-density region. For $\phi_2 > 0.5$, this simple quadratic formula is still more accurate than other more sophisticated calculations of ζ_2. The linear term of the quadratic formula is the dominant one. Using our simulation data for ζ_2, we compute three-point bounds on the conductivity σ_e and Torquato's approximation for σ_e.

I. INTRODUCTION

Prediction of effective material properties (e.g., transport, mechanical, and electromagnetic properties) of disordered composite media is a problem of considerable fundamental importance and has in recent years been the subject of numerous studies (see Refs. 1 and 2 and references therein). The ability to predict such properties from a knowledge of the microstructure is desireable from both the practical design and theoretical standpoints. However, to exactly predict such effective properties, an infinite set of correlation functions which statistically characterize the microstructure must be known. In practice, these correlation functions are never known, except in a very few special cases, making exact determination of the macroscopic property generally impossible for even the simplest of random models such as random arrays of parallel hard cylinders or hard spheres.

A useful alternative to predicting property values exactly is the determination of rigorous bounds on the properties which require only limited microstructural information. Rigorous upper and lower bounds are attractive in several respects: (1) they allow one to test the validity of a theory or computer-simulation result; (2) as more microstructural information is included, the bounds become progressively narrower; and (3) one of the bounds often provides relatively accurate estimates of the actual property value, even in the case where the reciprocal bound diverges from it. Thus, the calculation of bounds is of significant theoretical and practical value.

For two-phase isotropic composites, Hashin and Shtrikman[3] derived the best bounds on the effective thermal (or electrical) conductivity σ_e given just the phase volume fractions ϕ_1 and ϕ_2. Beran[4] and Torquato,[5] employing classical variational principles, have derived different but related *three-point* bounds on the conductivity of two-phase isotropic composites which improve upon the Hashin–Shtrikman bounds. Beran's bounds were derived using trial fields based on the first two terms of the exact "perturbation" expansion and thus were applicable to two-phase media of arbitrary topology. Torquato utilized trial fields based on the first two terms of the exact "cluster" expansion for a dispersion of spherical particles in a matrix to derive so-called cluster bounds. The three-point perturbation and cluster bounds incorporate *different* types of statistical correlation functions up to the three-point level.

Interestingly, for the special case of totally impenetrable spheres (i.e., hard spheres) dispersed in a matrix, the perturbation and cluster bounds have been shown to be identical[6] and depend upon a key microstructural parameter ζ_2. The quantity ζ_2 (defined below) is a multidimensional integral involving the three-point probability function $S_3(\mathbf{r}_1,\mathbf{r}_2,\mathbf{r}_3)$ which gives the probability of simultaneously finding three points at $\mathbf{r}_1$, $\mathbf{r}_2$, and $\mathbf{r}_3$ all in one phase, say the matrix phase. S_3 is a functional of the radial distribution function $g_2(r)$ and the three-particle distribution function $g_3(r_{12},r_{13},r_{23})$ for hard spheres.[7] Although $g_2(r)$ is known very accurately for hard spheres, g_3 for arbitrary sphere volume fraction ϕ_2 is known only approximately analytically. Beasley and Torquato[6] computed ζ_2 exactly through third order in ϕ_2 for an equilibrium distribution of hard spheres. Torquato and Lado[8] were the first to compute ζ_2 for such a model to all orders in ϕ_2 using the well-known Kirkwood superposition approximation for the three-particle distribution function:

$$g_3(r_{12},r_{13},r_{23}) \approx g_2(r_{12})g_2(r_{13})g_2(r_{23}). \quad (1)$$

a) Author to whom all correspondence should be addressed.

 0021-8979/90/235486-08$03.00

Recently, Blawzdziewicz and Stell[9] employed a more complicated but accurate approximation to g_3, called the "ladder" approximation, in order to compute the integral ζ_2. However, there are still no exact data for ζ_2 to all orders in ϕ_2 for the useful hard-sphere model and hence an assessment of the accuracy of the aforementioned approximations has not heretofore been possible.

As an alternative to analytical evaluation of the bounds, simulation techniques may be used to determine "exactly" the value of the multidimensional integral ζ_2. The resulting data can then be used as a benchmark to which the various theories and approximations may be compared. The purpose of this paper is to compute ζ_2 exactly for an *equilibrium* distribution of equisized hard spheres from Monte Carlo computer simulations and to use this information to determine three-point conductivity bounds exactly for the aforementioned microstructure.

In Sec. II the parameter ζ_2 is defined and related to the three-point cluster bound of Torquato. In Sec. III we describe the simulation technique used to compute ζ_2 for distributions of hard spheres. In Sec. IV we present results of the simulation and compare the data to several analytical calculations of ζ_2. Three-point bounds on the effective conductivity of a suspension of hard spheres using our evaluation of ζ_2 are also given. Here we also compute an accurate approximation of the conductivity for our model which depends on ζ_2. Finally, conclusions and comments are presented in Sec. V.

II. PERTURBATION AND CLUSTER BOUNDS

Beran[4] utilized the variational principles of minimum potential and minimum complementary potential energy to derive rigorous bounds on the effective conductivity σ_e of an isotropic composite medium composed of two phases having phase conductivities σ_1 and σ_2 and volume fractions ϕ_1 and ϕ_2. Beran utilized trial fields based upon the first two terms of certain perturbation expansions for the fields to obtain bounds later simplified by Torquato[10] and Milton.[11] These bounds on σ_e are given by

$$\left(\left\langle\frac{1}{\sigma}\right\rangle - \frac{4\phi_1\phi_2(1/\sigma_2 - 1/\sigma_1)^2}{6/\sigma_1 + (4\phi_1 + 2\zeta_2)(1/\sigma_2 - 1/\sigma_1)}\right)^{-1} \leqslant \sigma_e \leqslant \left(\langle\sigma\rangle - \frac{\phi_1\phi_2(\sigma_2 - \sigma_1)^2}{3\sigma_1 + (\phi_1 + 2\zeta_2)(\sigma_2 - \sigma_1)}\right), \tag{2}$$

where $\langle X\rangle = X_1\phi_1 + X_2\phi_2$ is the ensemble average of any property X. In the above equation, ζ_2 is a three-point microstructural parameter defined by the expression

$$\zeta_2 = 1 - \frac{1}{16\phi_1\phi_2\pi^2}\int\int d\mathbf{r}_{12}\, d\mathbf{r}_{13}\, \frac{P_2(\cos\theta)}{r_{12}^3 r_{13}^3} \times\left(S_3(r_{12},r_{13},r_{23}) - \frac{S_2(r_{12})S_2(r_{13})}{S_1}\right), \tag{3}$$

The quantities $S_2(r_{12})$ and $S_3(r_{12},r_{13},r_{23})$ are, respectively, the probabilities of finding in phase 1 the end points of a line segment of length r_{12} and the vertices of a triangle with sides of length r_{12}, r_{13}, and r_{23}; θ is the angle opposite the side of length r_{23} and P_2 is the Legendre polynomial of order two.

Taking a different approach, Torquato[5] used the first two terms from the cluster expansion and the same variational principles to derive three-point bounds on the effective conductivity of a dispersion of identical partially penetrable spherical particles. Specifically, the trial fields are taken to be a constant vector added to the sum of contributions from individual isolated spheres. Explicitly, the three-point cluster bounds are given by

$$\left(\langle 1/\sigma\rangle - \frac{\langle \mathbf{J}^{(1)}/\sigma\rangle\cdot\langle\mathbf{J}^{(1)}/\sigma\rangle}{\langle \mathbf{J}^{(1)}\cdot\mathbf{J}^{(1)}/\sigma\rangle}\right)^{-1} \leqslant \sigma_e \leqslant \left(\langle\sigma\rangle - \frac{\langle\sigma\mathbf{E}^{(1)}\rangle\cdot\langle\sigma\mathbf{E}^{(1)}\rangle}{\langle\sigma\mathbf{E}^{(1)}\cdot\mathbf{E}^{(1)}\rangle}\right), \tag{4}$$

where $\mathbf{E}^{(1)}$ is the trial electric field fluctuation defined below, $\mathbf{J}^{(1)}$ is the trial current field fluctuation, and angular brackets denote an ensemble average. The local conductivity can be expressed in terms of the conductivities of the characteristic function of the phase, i.e.,

$$\sigma(\mathbf{r}) = \sigma_1 I^{(1)}(\mathbf{r}) + \sigma_2 I^{(2)}(\mathbf{r}), \tag{5}$$

where

$$I^{(i)}(\mathbf{r}) = \begin{cases} 1, & \mathbf{r}\in D_i, \\ 0, & \text{otherwise}, \end{cases} \quad i = 1,2, \tag{6}$$

and D_1 and D_2 are the regions of space occupied by matrix and particles, respectively. For N spheres of radius a centered at positions $\mathbf{r}^N \equiv \mathbf{r}_1,\mathbf{r}_2,\ldots,\mathbf{r}_N$, respectively, it has been shown that[7]

$$I^{(1)}(\mathbf{r};\mathbf{r}^N) = \prod_{i=1}^{N}[1 - m(|\mathbf{r} - \mathbf{r}_i|)], \tag{7}$$

where

$$m(|\mathbf{r} - \mathbf{r}_i|) = \begin{cases} 1, & \text{if } |\mathbf{r} - \mathbf{r}_i| < a \\ 0, & \text{if } |\mathbf{r} - \mathbf{r}_i| > a, \end{cases} \tag{8}$$

where $\mathbf{r}_i$ is the position of the ith sphere, and $|\mathbf{r} - \mathbf{r}_i|$ is the position vector originating from the center of the ith sphere. For an inhomogeneous system of N spheres with one-body probability density $\rho_1(\mathbf{r})$, the trial fluctuation field $\mathbf{E}^{(1)}$ at any position $\mathbf{r}$ is given by[5]

$$\mathbf{E}^{(1)}(\mathbf{r};\mathbf{r}^N) = \sum_{i=1}^{N}\overline{\mathsf{K}}(\mathbf{x}_i)\cdot\langle\mathbf{E}\rangle - \int d\mathbf{r}_1\,\rho_1(\mathbf{r}_1)\overline{\mathsf{K}}(\mathbf{x}_1)\cdot\langle\mathbf{E}\rangle, \tag{9}$$

where $\overline{\mathsf{K}}$ is the single-body operator

$$\overline{\mathsf{K}}(\mathbf{r}) = \begin{cases} \beta a^3/r^3(3\hat{\mathbf{r}}\hat{\mathbf{r}} - \mathsf{U}), & r > a \\ -\beta\mathsf{U}, & r < a, \end{cases} \tag{10}$$

$\langle\mathbf{E}\rangle$ is the average field, and

$$\beta = \frac{\sigma_2 - \sigma_1}{\sigma_2 + 2\sigma_1}. \tag{11}$$

Here $\mathbf{x}_i = \mathbf{r} - \mathbf{r}_i$, $r = |\mathbf{r}|$, $\hat{\mathbf{r}} = \mathbf{r}/r$, and U is the unit dyadic. A similar expression has been given for $\mathbf{J}^{(1)}$.[5]

For the special case of statistically isotropic media, substitution of these relations into (4) has been shown to yield[5]

$$\left\{\left\langle\frac{1}{\sigma}\right\rangle-\left[4\phi_1^2\eta^2\left(\frac{1}{\sigma_2}-\frac{1}{\sigma_1}\right)^2\right]\Big/\left[\frac{2A}{\sigma_1}+(B+2\phi_1^2\phi_2)\left(\frac{1}{\sigma_2}-\frac{1}{\sigma_1}\right)\right]\right\}^{-1}$$
$$\leqslant\sigma_e\leqslant\left(<\sigma>-\frac{\phi_1^2\eta^2(\sigma_2-\sigma_1)^2}{\sigma_1 A+(\sigma_2-\sigma_1)B}\right), \tag{12}$$

where $\eta=4\pi\rho a^3/3$ is a reduced density, $\rho=\rho_1(\mathbf{r}_1)$ is a constant equal to the number density of the spheres of radius a, and $\langle\mathbf{E}\rangle$ is a constant vector. It is only for the special case of totally impenetrable spheres that $\eta=\phi_2$, i.e., the reduced density η is equal to the sphere volume fraction ϕ_2. The quantities A and B of (12) are integrals over the so-called point/n-particle distribution functions (see Ref. 5 for further details). Note that the form of (9) ensures the absolute convergence of the integrals A and B (Ref. 5).

As noted earlier, the Beran and Torquato bounds have been shown to be identical for dispersions of identical hard spheres. Comparison of Eq. (12) with Beran's upper bound [Eq. (2)] yields

$$A=3\phi_1\phi_2 \tag{13}$$

and

$$B=\phi_1^2\phi_2+2\zeta_2\phi_1\phi_2. \tag{14}$$

In light of the relation[5]

$$\sigma_1 A+(\sigma_2-\sigma_1)B=\frac{\langle\sigma\mathbf{E}^{(1)}\cdot\mathbf{E}^{(1)}\rangle}{\beta^2\langle\mathbf{E}\rangle\cdot\langle\mathbf{E}\rangle}, \tag{15}$$

it is easily shown that

$$\zeta_2=\frac{\langle I^{(2)}\mathbf{E}^{(1)}\cdot\mathbf{E}^{(1)}\rangle}{2\phi_1\phi_2\beta^2\langle\mathbf{E}\rangle\cdot\langle\mathbf{E}\rangle}-\frac{\phi_1}{2}. \tag{16}$$

The above expression relates ζ_2 to the average of $I^{(2)}\mathbf{E}^{(1)}\cdot\mathbf{E}^{(1)}$, where $\mathbf{E}^{(1)}$ is the sum of particle interactions as defined by Eq. (9). Use of relation (9) for $\mathbf{E}^{(1)}$ reveals that the right-hand side of (16) is independent of both σ_i and $\langle\mathbf{E}\rangle$ and hence is a purely microstructural quantity dependent on ϕ_2 only, as expected. Equations (3) and (16) then provide two independent means of determining ζ_2, either of which may be used as the basis for Monte Carlo simulations.

Smith and Torquato[12] employed the two-dimensional form of Eq. (3) to directly simulate ζ_2 in two dimensions by sampling $S_3(r_{12},r_{13},r_{23})$ for a random array of circular disks and numerically evaluating the two-dimensional integral analagous to Eq. (3). By employing Gaussian quadrature, the values of r_{12}, r_{13}, and r_{23} were fixed according to the value of the Gaussian points of the integration order used. A triangular sampling template with sides r_{12}, r_{13}, and r_{23} was randomly placed over the configuration and rotated at equal angular intervals about one vertex to sample S_3. These simulated values of S_3 were then integrated to determine ζ_2.

To employ this method in three dimensions would require an order of magnitude more computation time to adequately sample S_3. In two dimensions, each template is rotated in a circle about one of the vertices which falls in phase 1. In three dimensions, however, each template must be rotated through a sphere, requiring a much longer sampling time for each integration point.

Equation (16) provides us with a different means to determine ζ_2 which does not require direct sampling of the three-point probability function S_3. Instead (16) enables one to perform summations over particle interactions. Taking this approach to the simulation greatly reduces the sampling time required, allowing a much more efficient simulation algorithm for determination of ζ_2.

A highly accurate approximation of σ_e for dispersions derived by Torquato[13] also depends upon the three-point parameter ζ_2. (This approximation is fully described in Sec. IV.) Thus precise determination of ζ_2 for hard spheres will enable us to evaluate this approximation for σ_e with heretofore unattained accuracy and will be used to assess the sharpness of the three-point bounds.

III. SIMULATION TECHNIQUE

Simulation of ζ_2, as defined through Eq. (16), is a straightforward process given the relatively simple expression for $\mathbf{E}^{(1)}$ in Eq. (9). The simulation process itself is composed of two primary steps: the first being to generate an *equilibrium* distribution of spheres, and the second to sample for the quantity of interest over a sufficient number of configurations.

A. Generation of equilibrium configurations

To generate an equilibrium configuration, a standard Metropolis algorithm is used.[14] Spheres are initially placed in a periodic array with no overlap in a cubic cell of side L with number density ρ. This cell is surrounded by periodic images of itself. Each particle is then moved a small distance to a new position, and the move is accepted or rejected according to whether it overlaps with an adjacent sphere. This process is repeated until equilibrium is achieved. Typically, each particle is moved up to 400 times before the initial equilibrium configuration is reached. After sampling a configuration for ζ_2, each particle is moved up to 80 times to generate a different equilibrium configuration.

In order to ensure that equilibrium is achieved, the simulation program measures the contact value of the pair or radial distribution function $g_2(d)$, $d=2a$, which is trivially related to the pressure of the system. [The quantity $4\pi r^2\rho g_2(r)dr$ gives the conditional probability of finding a sphere at a radial distance r in the volume $4\pi r^2\,dr$, given that there is a sphere at the origin.] The contact value of g_2 is then compared to previously obtained accurate estimates of it. For values of the sphere volume fraction $\phi_2\leqslant 0.5$, we compare $g_2(d)$ to the well-known Carnahan–Starling approximation.[15] For values of $0.5<\phi_2<0.6$, (i.e., sphere volume fractions between 64% and 95% of random close packing for hard spheres, $\phi_2\approx 0.63$) the series expression of Song, Stratt, and Mason[16] is used as a comparison. For $\phi_2=0.5$, 0.55, and 0.6, we found $g_2(d)=6.01$, 11.01, and 22.90, respectively, all of which are in very good agreement with the aforementioned results[15,16] [$g_2(d)=6.00$, 10.45, and 23.24] in this difficult region (see discussion below). Not only were the contact values for each run determined, but values of $g_2(r)$ for other values of r were also sampled for

$r \leqslant L/2$, (i.e., half the length of the central cell). The sampled radial distribution function g_2 for all r agreed well with previous results.[17] In particular, the behavior of the distribution function at $\phi_2 = 0.5$ was in excellent agreement with that reported in Ref. 17 for a system near freezing density ($\phi_2 \approx 0.497$). For sphere volume fractions above this value, generation of equilibrium configurations becomes quite difficult due to the metastable behavior of the hard-sphere fluid in this region. For $\phi_2 > 0.5$, equilibrium configurations were achieved by first generating a random array at $\phi_2 = 0.5$, then allowing the particles to "swell" (i.e., increase the diameter) slightly to reach the higher volume fraction desired. If a "swelled" particle overlaps another particle, then it is moved a very small distance to find adequate space to swell. If no free space can be found after ten attempts, the entire configuration is "jiggled" by randomly moving each particle (at its larger diameter) a small distance. The process is repeated until each particle is swelled. The radial distribution function for all r at $\phi_2 = 0.55$ agreed well with the data for $g_2(r)$ reported by Woodcock.[17] It was noticed that the current simulation results for g_2 produced the interesting subpeaks observed by Woodcock for a rapidly quenched glass at a distance of $r/2a \approx 2$. The good agreement with previous results for $g_2(r)$ for both the contact values and the other values of r confirm that the configurations generated are indeed equilibrium in nature, which allows a valid comparison between the simulated data for ζ_2 and those determined analytically.

B. Sampling for ζ_2

After an equilibrium configuration has been generated, images of the configuration are placed around the central cell to approximate an infinite system. The total number of particles N is given by

$$N = N_c N_i, \tag{17}$$

where N_c is the number of spheres in the central cell and N_i is the number of image cells. The number of image cells that we employ varies depending upon the size of the central cell. The size of the central cell varies roughly from $L = 4d$ to $5d$, depending on the particular value of the sphere volume fraction ϕ_2 desired. Since $\mathbf{E}^{(1)}$ is a relatively short-ranged function of r, as seen by the r^{-3} dependence of $\overline{K}$ in Eq. (10), the number of image cells N_i, for fixed ϕ_2, may be decreased as the size of the central cell increases (or equivalently as N_c increases). Thus for $\phi_2 \leqslant 0.4$, the total system is composed of 125 identical cells (including the central cell), while for $\phi_2 > 0.4$, the total system requires only 27 identical cells. For $\phi_2 < 0.4$, $N = 2000$, at $\phi_2 = 0.4$, $N = 6250$, and for $\phi_2 > 0.4$, $N = 3024$.

Once the system has been generated, one can then sample for the value of the trial fluctuation field $\mathbf{E}^{(1)}$ as given by Eq. (9). First, a point is chosen at random within the central cell. The value of $\overline{K}$ is then calculated for each of the N spheres in the system, according to Eq. (10). In addition, the local conductivity $\sigma(\mathbf{r})$ is determined by Eq. (5), according to whether the sample point has fallen inside or outside a sphere. Each sphere in the central cell as well as those in the periodic image cells contributes to $\mathbf{E}^{(1)}$. After all N spheres have been sampled, the quantity $I^{(2)}\mathbf{E}^{(1)}\cdot\mathbf{E}^{(1)}$ is calculated, and the next sample point is chosen. [Recall $I^{(2)}$ is the particle-phase characteristic function–see Eq. (7).] This is repeated for a sufficiently large number of sample points. A new configuration is then generated, and the sampling described above is repeated for the new configuration. The quantity $\langle I^{(2)}\mathbf{E}^{(1)}\cdot\mathbf{E}^{(1)}\rangle$ represents an average over 1500–3000 configurations and 5000 sample points per configuration for each value of ϕ_2 reported. ζ_2 is then determined by use of Eq. (16). Simulations were carried out on both the DEC station 3100 and CRAY Y-MP.

IV. RESULTS AND DISCUSSION

A. Microstructural parameter ζ_2

As a check on the accuracy of the simulation procedure, the method was first used to simulate ζ_2 for a simple cubic array of identical spheres; for this model ζ_2 is known exactly.[18] The system was composed of a simple cubic array of particles, each in the center of a cube of unit length ($N_c = 1$). The diameter of each particle was determined by the desired sphere volume fraction. As a test, five separate system sizes ranging from $N = 3^3$ to $N = 11^3$ were used, where N denotes the total number of particles in the simple cubic array. These runs were then compared to determine the effect of system size on the simulation of ζ_2. The results of this study are shown in Table I. Even the smallest system size produced an error of less than 7% over three runs, while an error of less than 1% was obtained with a system size of $N = 7^3$. For $N = 11^3$, the simulation showed excellent agreement with exact numerical values of ζ_2 previously reported,[18] confirming the validity and accuracy of the simulation method. For a sphere volume fraction of $\phi_2 = 0.4$, the simulation results were within 0.02% of the tabulated values. In every instance, the simulated value of ζ_2 was less than the exact value: the difference decreasing with increasing N. This is consistent with the fact that the simulation procedure necessarily samples a large but finite system rather than a true infinite system. Each simulation point represents three separate runs of 50 000 sample points. The runs were made on a DEC station 3100, and CPU times for each run varied from just over 100 min for the largest system size to just over 2 min for the smallest.

Before presenting results of the simulations for random arrays, it is useful to examine some previous results for ζ_2 of equilibrium distributions of impenetrable spheres. Felderhof[19] first calculated ζ_2 for this model through third order in

TABLE I. Effect of system size N on the simulation results for ζ_2 for a simple cubic array of spheres at $\phi_2 = 0.4$. The simulation values are compared to $\zeta_2 = 0.068$ (see Ref. 18).

N	ζ_2	% error
11	0.06799	−0.02
9	0.06781	−0.28
7	0.06746	−0.79
5	0.06618	−2.03
3	0.06347	−6.66

TABLE II. Results for the three-point microstructural parameter ζ_2 of equilibrium distributions of identical impenetrable spheres.

ϕ_2	Simulation results	Quadratic formula (20)	Linear formula (19)	Superposition approximation results[a]	Ladder approximation results[b]
0.10	0.0199	0.02060	0.02107	0.02060	0.0204
0.20	0.0409	0.04026	0.04214	0.03983	0.0390
0.30	0.0597	0.05898	0.06320	0.05875	0.0550
0.40	0.0765	0.07676	0.08427	0.08356	0.0681
0.50	0.0938	0.09361	0.1053	0.1407	0.0790
0.55	0.109	0.10168	0.1159	0.2051	0.0847
0.60	0.134	0.10951	0.1264	0.3277	0.0937

[a] Reference 8.
[b] Reference 9.

ϕ_2 in the superposition approximation [Eq. (1)]. Beasley and Torquato[6] computed ζ_2 exactly through third order in ϕ_2 for this model and found

$$\zeta_2 = 0.21068\phi_2 - 0.04693\phi_2^2 + 0.00247\phi_2^3. \tag{18}$$

They found that ζ_2 as derived using the superposition approximation (here denoted by ζ_2^{sa}) underestimated the exact value of ζ_2 through order ϕ_2^3. Torquato and Lado[8] calculated ζ_2 to all orders in the sphere volume fraction (i.e., up to about 94% of the random-close-packing value) in the superposition approximation. However, recent work by Blawzdziewicz and Stell[9] which uses the more accurate ladder approximation for g_3 indicates, that at *high* values of ϕ_2, ζ_2 is actually less than ζ_2^{sa}.

In Table II and Fig. 1, we summarize our simulation results for ζ_2 and compare them to the previous results of Refs. 8 and 9 and to the linear and quadratic formulas,

$$\zeta_2 = 0.21068\phi_2 \tag{19}$$

and

$$\zeta_2 = 0.21068\phi_2 - 0.04693\phi_2^2, \tag{20}$$

respectively, which are simply Eq. (18) truncated after one and two terms. Remarkably, the quadratic formula (20), exact to second order in ϕ_2, follows the simulation data very closely up to and including $\phi_2 = 0.5$, which, as noted earlier, is very slightly above the value of the fluid-solid phase transition. This indicates that third- and higher-order terms are negligibly small. Note that the linear term of (20) is actually the dominant one as evidenced by the fact that the linear formula (19), although not as accurate as the quadratic formula (20), is a good approximation to the data for $\phi_2 \leqslant 0.5$.

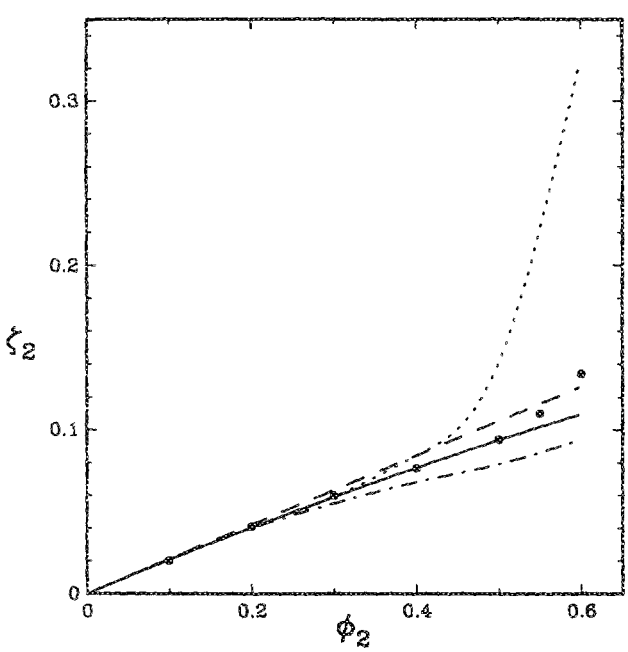

FIG. 1. Three-point parameter ζ_2 for equilibrium dispersions of impenetrable spheres. The large black circles (●) denote values of ζ_2 as calculated from the simulation using Eq. (16), the dotted line (···) indicates ζ_2 as calculated using the superposition approximation (see Ref. 8), the dashed line (- - -) is the linear formula (19), the solid line (—) is the quadratic formula, Eq. (20), and the dashed and dotted line (-·-·-) indicates ζ_2 as calculated using the ladder approximation (see Ref. 9).

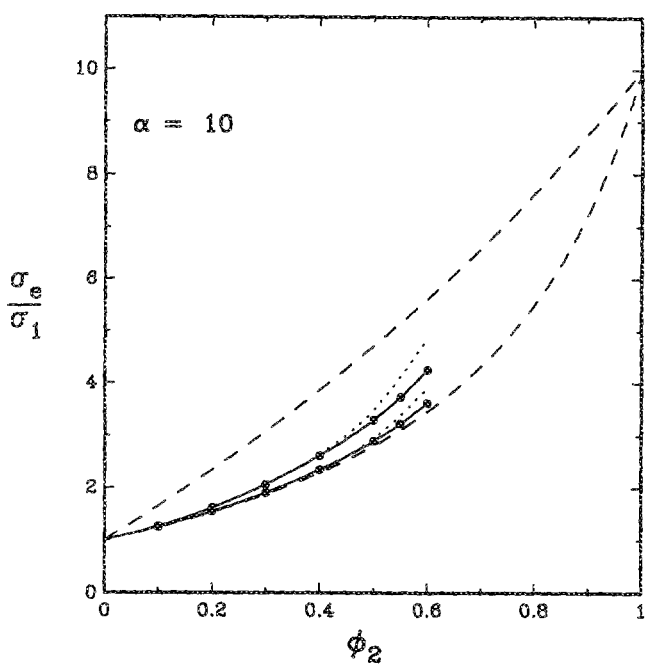

FIG. 2. Upper and lower bounds on the reduced effective conductivity σ_e/σ_1 vs ϕ_2 for equilibrium dispersions of impenetrable spheres at $\alpha = \sigma_2/\sigma_1 = 10$. The large black circles (●) indicate values of the three-point Beran upper bound [Eq. (2)] and the Milton lower bound [Eq. (21)] calculated from our simulation results of ζ_2. The solid lines (—) are spline fits of the simulation data. The dashed lines (- - -) are the two-point Hashin–Shtrikman bounds (see Ref. 3). The dotted lines (···) are the Beran upper bound and the Milton lower bound as calculated using ζ_2 in the superposition approximation (see Ref. 8).

The important significance of these results shall be discussed below. For $0.5 \leqslant \phi_2 \leqslant 0.54$, values in the metastable region, the quadratic formula (20) still provides the closest agreement with the data. For $0.54 \leqslant \phi_2 \leqslant 0.6$, the linear formula (19) is the most accurate, with the quadratic formula (20) being the next most accurate calculation. For the range $0 \leqslant \phi_2 \leqslant 0.4$, the superposition-approximation results[8] are more accurate than the ladder approximation.[9] On the other hand, for $\phi_2 \geqslant 0.5$, the ladder approximation is superior to the corresponding superposition-approximation results which significantly overestimate ζ_2.

It is useful to discuss the significance of the fact that exact low-density expansions of ζ_2 provide very good agreement with the simulation data for a wide range of ϕ_2. First, this should not come as any great surprise since Torquato and Lado[8] have already observed that ζ_2 is either exactly or approximately linear in ϕ_2 for a variety of different sphere distributions, including symmetric-cell materials,[20] fully penetrable or overlapping spheres,[21,22] and totally impenetrable spheres. (Symmetric-cell materials are constructed by tessellating space into "cells" of various shapes and sizes, with cells randomly and independently designated as phase 1 or phase 2 with probabilities ϕ_1 and ϕ_2, respectively.) Thovert *et al.*[23] and Torquato[24] have already exploited the linear approximation for ζ_2 in order to compute the three-point bounds on the effective conductivity and thermoelastic properties, respectively, for impenetrable spheres with a polydispersivity in size for a wide range of ϕ_2. Torquato[21] has shown that the first-order coefficient of (20) depends on the zero-density limit of the pair distribution function g_2 for distributions of particles. Similarly, the quadratic term of (20) depends on g_2 to first order in ϕ_2 and the zero-density limit of the triplet distribution function g_3.[8,19,25] Thus, the high accuracy that the quadratic formula (20) provides, even at high volume fractions, indicates that ζ_2, for this wide range of ϕ_2, only incorporates essentially up to *three-body* effects to *lowest order*: a result consistent with the fact that ζ_2 contains little information about the many-body phenomenon of percolation. Based upon the discussion above, this is expected to be true for general statistically isotropic two-and three-dimensional distributions of disks and spheres, respectively, with a polydispersivity in size and an arbitrary degree of penetrability. This is a very practically useful conclusion since the exact calculation of ζ_2 through second order in ϕ_2 for distributions of impenetrable particles is much easier to arrive at than the corresponding full-density dependent calculation which necessarily involves the use of some approximation for g_3 whose validity is usually questionable at high densities.

Let us remark on the behavior of closely related three-point microstructural parameters. First, it is known[2] that ζ_2 for three-dimensional distributions of particles is functionally very similar to the corresponding two-dimensional analog of ζ_2 for isotropic distributions of particles. Second, it is also clear from the work of Sen, Lado, and Torquato[26] that a different microstructural parameter η_2, which arises in three-point bounds on the effective shear modulus of two-phase composites,[11,27] also shows the same general features as ζ_2 for two- and three-dimensional distributions of particles. Accordingly, the exact expansions of all the aforementioned three-point parameters through second order in ϕ_2 for such microgeometries should yield accurate estimates of them for a wide range of ϕ_2.

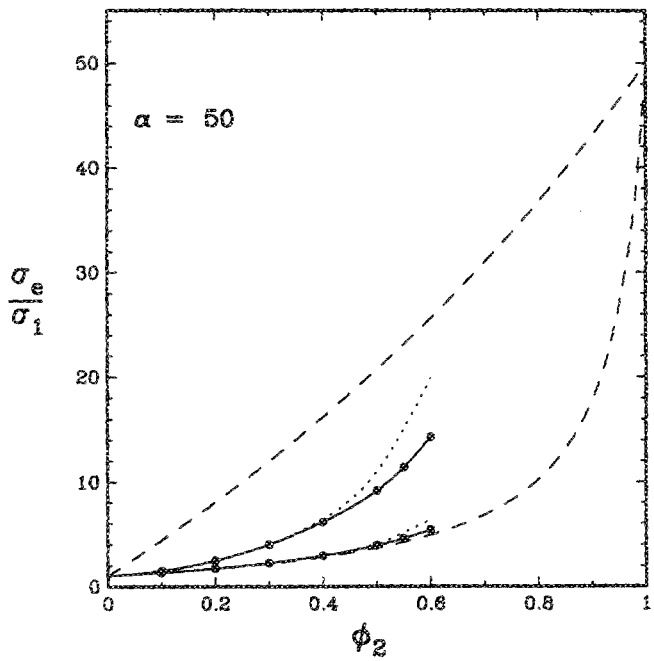

FIG. 3. As for Fig. 2 with $\alpha = 50$.

Finally, the maximum error in the simulation data for ζ_2 given in Table II should occur at the smallest volume fraction reported, i.e., at $\phi_2 = 0.1$. Thus, the maximum per-

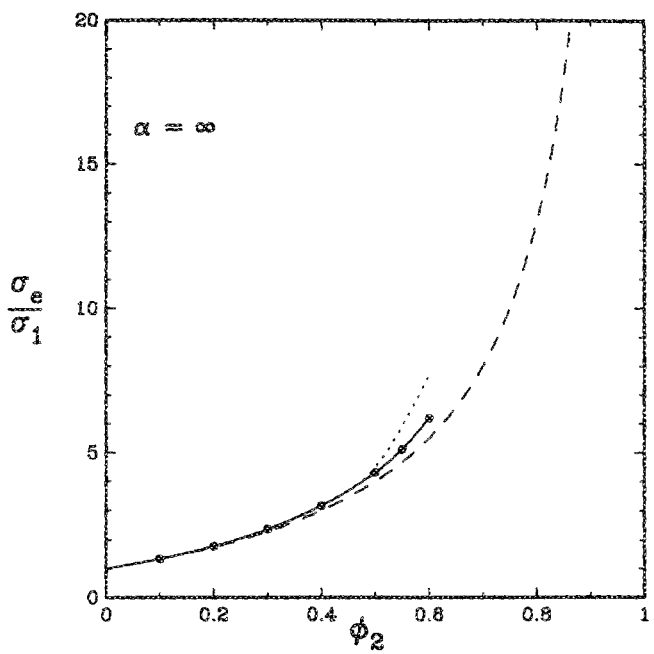

FIG. 4. Lower bounds on the reduced effective conductivity σ_e/σ_1 vs ϕ_2 for equilibrium dispersions of superconducting impenetrable spheres ($\alpha = \infty$). The large black circles (●) indicate values of the three-point Milton lower bound {Eq. (21)} calculated from our simulation results for ζ_2. The solid lines (—) are spline fits of the simulation data. The dotted line (···) is Milton's bound calculated from ζ_2 in the superposition approximation (see Ref. 8). The dashed line (- - -) is the two-point Hashin–Shtrikman lower bound (see Ref. 3).

centage error can easily be estimated since ζ_2 is essentially exact for such ϕ_2 from either the quadratic formula (20), superposition approximation[8] or the ladder approximation.[9] Accordingly, the error in ζ_2 at $\phi_2 = 0.1$ is approximately 3%.

B. Conductivity bounds

Given the values of ζ_2 from our simulations, it is now possible to calculate three-point upper and lower bounds on the conductivity from Eq. (2) for arbitrary values of $\alpha = \sigma_2/\sigma_1$ and volume fraction ϕ_2. For the case $\zeta_2 = 1$, the bounds (2) coincide with the two-point Hashin–Shtrikman[3] upper bound for $\sigma_2 \geqslant \sigma_1$ (i.e., $\alpha \geqslant 1$). In the opposite case of $\zeta_2 = 0$, the Beran bounds on σ_e coincide with the Hashin–Shtrikman lower bound for $\sigma_2 \geqslant \sigma_1$. The fact that ζ_2 lies in the interval [0,1] implies that the three-point Beran bounds (2) always improve on the two-point Hashin-Shtrikman bounds.

For $\alpha \geqslant 1$, Milton[28] derived the following three-point lower bound on σ_e

$$\frac{\sigma_e}{\sigma_1} \geqslant \frac{(1+2\alpha)(\alpha+2\phi_1+2\alpha\phi_2)+2\phi_1\zeta_2(\alpha-1)^2}{(1+2\alpha)(2+\phi_2+\alpha\phi_1)+2\phi_1\zeta_2(\alpha-1)^2}. \tag{21}$$

Since bound (21) is the best possible lower bound on σ_e given σ_1, σ_2, ϕ_2, and ζ_2,[28] we shall utilize it in our calculations instead of the three-point lower bound of (2). Note, however, that the improvement of (21) over the Beran bound of (2) is very small.[8]

Milton's lower bound (21) and the Beran upper bound (2) are calculated and plotted in Figs. 2–4 for random hard-sphere dispersions using our simulation data for ζ_2. Included in the figures are the corresponding three-point bounds computed by Torquato and Lado[8] in the superposition approximation and the two-point Hashin–Shtrikman bounds.[3] Consistent with the previous conclusions of Torquato and Lado for this model, it is observed that the three-point bounds generally provide significant improvement over the two-point bounds for $\alpha = 10$ and $\alpha = 50$, i.e., provided α is not very large ($\alpha \gg 1$). As expected, at large ϕ_2, the superposition approximation results generally overestimate, to varying degrees, the three-point bounds on σ_e. In the case of superconducting spheres relative to the matrix, $\alpha = \infty$ (see Fig. 4), the upper bounds, not surprisingly, diverge to infinity and hence only the lower bounds remain finite. Nonetheless in such instances, the lower bounds will provide a reasonable estimate of the true effective conductivity σ_e since the particles never form clusters for the range of volume fractions studied here.[13]

To further illustrate this last point, we compare the highly accurate approximation

$$\frac{\sigma_e}{\sigma_1} \approx \frac{1+2\phi_2\beta-2\phi_1\zeta_2\beta^2}{1-\phi_2\beta-2\phi_1\zeta_2\beta^2} \tag{22}$$

developed for dispersions by Torquato[13] to the two- and three-point lower bounds for the case of superconducting spheres ($\alpha = \infty$) in Fig. 5. Here

$$\beta = \frac{\sigma_2-\sigma_1}{\sigma_2+2\sigma_1}. \tag{23}$$

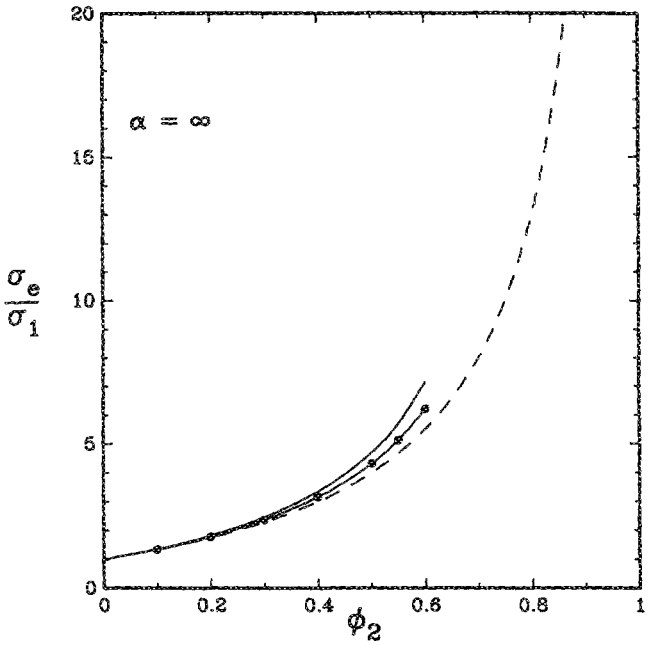

FIG. 5. Comparison of the accurate approximation (22) for the reduced effective conductivity σ_e/σ_1 for equilibrium dispersions of superconducting impenetrable spheres ($\alpha = \infty$), shown as a solid line (—), to the two-point Hashin–Shtrikman lower bound (- - -) and the three-point Milton lower bound [solid lines are spline fits of our simulation data shown as black circles (●)]. The curve generated from relation (22) is a spline fit of the points which result by use of our simulation data for ζ_2.

Relation (22), in the case $\alpha > 1$, has been shown[13] to yield an excellent estimate of σ_e for dispersions for all $\alpha (1 \leqslant \alpha \leqslant \infty)$, provided that the conducting particles do not form large clusters. This has recently been confirmed for the impenetrable-sphere model studied here by Kim and Torquato[29] who determined σ_e exactly from Brownian motion computer simulations. Thus, expression (22) (in conjunction with our simulation data for ζ_2) may be regarded as essentially exact "data" for an equilibrium distribution of equisized impenetrable spheres. Figure 5 indeed demonstrates that the three-point lower bound is a relatively good estimate of the effective conductivity.

V. CONCLUSIONS

Using an efficient simulation technique, we have computed the key microstructural parameter ζ_2 which arises in three-point conductivity bounds and in the accurate approximation (22) for the effective conductivity of an equilibrium distribution of hard spheres in a matrix for virtually the entire range of allowable volume fractions. An important and interesting finding is the fact that the simple quadratic formula, Eq. (20), has been shown to provide the best agreement with the simulation data for almost the entire volume-fraction range studied here, with the linear term being the dominant one. The calculation of ζ_2 in the superposition approximation has been shown to overestimate it at high sphere volume fraction ϕ_2, confirming the general conclusions of Blawzdziewicz and Stell.[9]

ACKNOWLEDGMENTS

The authors gratefully acknowledge the support of the Office of Basic Energy Sciences, U.S. Department of Energy, under Grant No. DE-FG05-86ER13482. This research was also supported by NASA Grant No. NAGW-1331 to the Mars Mission Research Center, which is a cooperative effort of North Carolina State University and North Carolina A & T State University. Some computer resources (CRAY Y-MP) were supplied by the North Carolina Supercomputing Center funded by the State of North Carolina.

[1] Z. Hashin, J. Appl. Mech. **50**, 481 (1983).
[2] S. Torquato, Rev. Chem. Eng. **4**, 151 (1987).
[3] Z. Hashin and S. Shtrikman, J. Appl. Phys. **23**, 779 (1962).
[4] M. Beran, Nuovo Cimento **38**, 771 (1965).
[5] S. Torquato, J. Chem. Phys. **84**, 6345 (1986).
[6] J. D. Beasley and S. Torquato, J. Appl. Phys. **60**, 3576 (1986).
[7] S. Torquato and G. Stell, J. Chem. Phys. **77**, 2071 (1982); **82**, 980 (1985).
[8] S. Torquato and F. Lado, Phys. Rev. B **33**, 6248 (1986).
[9] Results given by G. Stell, in *Lectures in Applied Mathematics*, edited by B. White and W. Kohler (American Mathematical Society, Rhode Island, in press). Details to be published by J. Blawzdziewicz and G. Stell.
[10] S. Torquato, Ph. D. dissertation, State University of New York at Stony Brook, 1980; see also S. Torquato and G. Stell, Lett. Appl. Eng. Sci. **23**, 375 (1985).
[11] G. W. Milton, Phys. Rev. Lett. **46**, 542 (1981).
[12] P. A. Smith and S. Torquato, J. Appl. Phys. **65**, 893 (1989).
[13] S. Torquato, J. Appl. Phys. **58**, 3790 (1985).
[14] N. Metropolis, A. W. Rosenbluth, M. N. Rosenbluth, A. N. Teller, and E. Teller, J. Chem. Phys. **21**, 1087 (1953).
[15] N. F. Carnahan and K. E. Starling, J. Chem. Phys. **51**, 635 (1969).
[16] Y. Song, R. M. Stratt, and E. A. Mason, J. Chem. Phys. **88**, 1126 (1988).
[17] L. V. Woodcock, Ann. N. Y. Acad. Sci. **371**, 274 (1981).
[18] R. C. McPhedran and G. W. Milton, Appl. Phys. **26**, 207 (1981).
[19] B. U. Felderhof, J. Phys. C **15**, 3953 (1982).
[20] M. Miller, J. Math. Phys. **10**, 1988 (1969).
[21] S. Torquato, J. Chem. Phys. **83**, 4776 (1985).
[22] J. G. Berryman, J. Phys. D **18**, 585 (1985).
[23] J. F. Thovert, I. C. Kim, S. Torquato, and A. Acrivos, J. Appl. Phys. **67**, 6088 (1990).
[24] S. Torquato, J. Appl. Phys. **67**, 7223 (1990).
[25] S. Torquato and F. Lado, Proc. R. Soc. London Ser. A **417**, 59 (1988).
[26] A. K. Sen, F. Lado, and S. Torquato, J. Appl. Phys. **62**, 4135 (1987).
[27] G. W. Milton, J. Mech. Phys. Solids **30**, 177 (1982).
[28] G. W. Milton, J. Appl. Phys. **52**, 5294 (1981).
[29] I. C. Kim and S. Torquato, J. Appl. Phys. (in press).